

Electrochromic properties of pure and doped Nb₂O₅ coatings and devices

M. Schmitt¹, M.A. Aegerter*

Institut für Neue Materialien gem. GmbH, INM, Im Stadtwald, Gebäude 43, D-66123 Saarbrücken, Germany

Received 21 August 2000; received in revised form 25 October 2000

Abstract

Coatings of pure and Zr, Sn, Li, Ti and Mo doped niobium pentoxide have been prepared by the sol-gel process and deposited on ITO-coated glass using the dip coating technique. Their structure, morphology and electrochromic (EC) properties have been studied. The coatings are transparent and, depending on the nature and amount of the doping and the sintering temperature, they present a brown, gray or blue color after Li insertion. The EC properties of 4 × 8 cm² size coatings, tested up to 5000 cycles, are highly stable with a coloration efficiency measured at 550 nm ranging between 16 and 28 cm²/C. Same size devices have been built with the configuration glass/FTO/pure or doped Nb₂O₅/liquid electrolyte/TiO₂-CeO₂/FTO/glass. In agreement with a theoretical estimation and with this choice of counterelectrode (IS), only Nb₂O₅:0.4 Mo coatings could be considered. For a fixed thickness (180 nm) of the IS electrode, the transmittance response of the device was found to increase with the thickness of the EC layer. The maximum change of the photopic transmission was 0.3 with an Li⁺ charge exchange of 18 mC/cm². The devices were stable up to about 15,000 potentiostatic cycles performed between ± 2.5 V, 120 s.

Keywords: Nb₂O₅ coating; Electrochromism; Device; Sol-gel

1. Introduction

In the last 15 years, the advent of sophisticated methods of preparation has made it possible to obtain, in a controlled way, pure and doped niobium pentoxide (Nb₂O₅) in the form of highly porous materials, very fine powders and coatings. Such materials have been used for the development of innovative devices such as batteries and nanocrystalline solar cells and in the field of catalysis and electrochromism [1]. One of these meth-

ods, the sol-gel process, is particularly useful for obtaining pure and doped oxide films of high optical quality whose structural properties (phases, porosity, etc.) can be easily tailored during the sintering step.

Pure Nb₂O₅ has been known as an electrochromic material (EC) since 1980 and coatings have been obtained by CVD, DC magnetron sputtering, electrochemical deposition and the sol-gel process (see references in Ref. [1]). A common feature of these coatings is their blue color observed under reversible Li⁺-ions insertion.

This paper presents a study of the structure, morphology and EC properties of pure and Sn, Zr, Li, Ti and Mo doped Nb₂O₅-coating obtained by the sol-gel process and sintered between 450 and 600°C. Complete EC cells using these materials as coloring electrode and sol-gel CeO₂-TiO₂ layer as IS electrode is also reported.

* Corresponding author. Tel.: +49-681-9300-317; fax: +49-681-9300-249.

E-mail address: aegerter@inm-gmbh.de (M.A. Aegerter).

¹ Present address. DIN Deutsches Institut für Normung e.V., Normenausschuß Materialprüfung (NMP), Burggrafentraße 6, D-10787 Berlin, Germany.

2. Experimental

All films were prepared using the sol–gel process [2]. A 0.4 M niobium solution was prepared by dissolving NbCl_5 (ChemPur) in ethanol and acetic acid. The doping was obtained by dissolving, in ethanol, SnCl_4 for Sn, ammonium zirconate for Zr, LiCF_3SO_3 for Li, titanium isopropoxide for Ti or phosphormolybdenum acid for Mo (all from Fluka). Both solutions were mixed and then subjected to an ultrasonic treatment during 2 min. All solutions were transparent.

The coatings have been deposited on $4 \times 8 \text{ cm}^2$ ITO-coated borosilicate glass (Asahi Glass, $10 \Omega_{\square}$) by the dip coating technique at a withdrawal rate of 2 mm/s. The films were then dried at room temperature and sintered in a two-step heat treatment at 100 and 450°C during 30 min. The whole procedure was repeated two times to increase the thickness of the coating. The resulting coating was finally sintered at temperature ranging between 400 and 600°C. Their thickness was measured using a Tencor P-10 profilometer.

Differential thermal analysis (DTA), thermo gravimetric (TG) and mass spectroscopy (MS) analysis of the effluents were performed simultaneously using a ST501 Bähr equipment at a rate of 10 K/min coupled to a mass spectrometer (Thermolab 1165 Fisons Instruments). The structure was determined by X-ray diffraction measurements performed at glancing incidence using a Siemens D 500 equipment with CuK_α radiation. The crystallite size was determined using the Siemens software (Diffrac AT V 3.1).

The electrochemical and in situ optical measurements were realized using an EG&G 270 A potentiostat (Princeton Applied Research) and a three-electrode cell. The two opposite sides of the cell were closed by the

working electrode and a quartz window. The counterelectrode was a platinum foil and the reference electrode was a 0.01 M solution of Ag/AgClO_4 dissolved in the used electrolyte. The electrolyte was a 1 M solution of LiClO_4 dissolved in propylene carbonate (PC). The intercalation/deintercalation of the lithium ions was studied by voltammetry (scan rate: 50 mV/s) and chronoamperometry (Li^+ insertion and deintercalation for 120 s between -2.2 and $+1.0$ V vs. Ag/AgClO_4).

The transmission spectra in the ultraviolet–visible–near-infrared (UV–Vis–NIR) range were recorded in situ with a CARY 5E spectrophotometer (Varian) in the bleached and colored states (T_{bleached} , T_{colored}). The change of optical density was calculated according to $(\Delta\text{OD} = -\log_{10}(T_{\text{bleached}}/T_{\text{colored}}))$.

Complete $8 \times 4 \text{ cm}^2$ cells have been built with the configuration substrate/ $\text{Nb}_2\text{O}_5\text{:X}$ /electrolyte/ $\text{CeO}_2\text{--TiO}_2$ /substrate. Commercial Libbey Owens Ford FTO-coated glass with $R_{\square} = 17 \Omega_{\square}$ were used as substrate. A 1 M solution of LiClO_4 in propylene carbonate was used as liquid electrolyte. Its thickness was about 1 mm. The IS layer or counterelectrode was prepared according to Ref. [3]. The light transmittance change $\Delta\tau$ (photopic response) of the cell was calculated according to DIN EN 410.

3. Results and discussion

3.1. EC coatings

A typical DTA-TG analysis obtained for a pure Nb_2O_5 xerogel (ethanolic sol) dried at 100°C is shown in Fig. 1. An exothermic peak is observed at 250°C. As it is accompanied by a large mass loss mainly involving

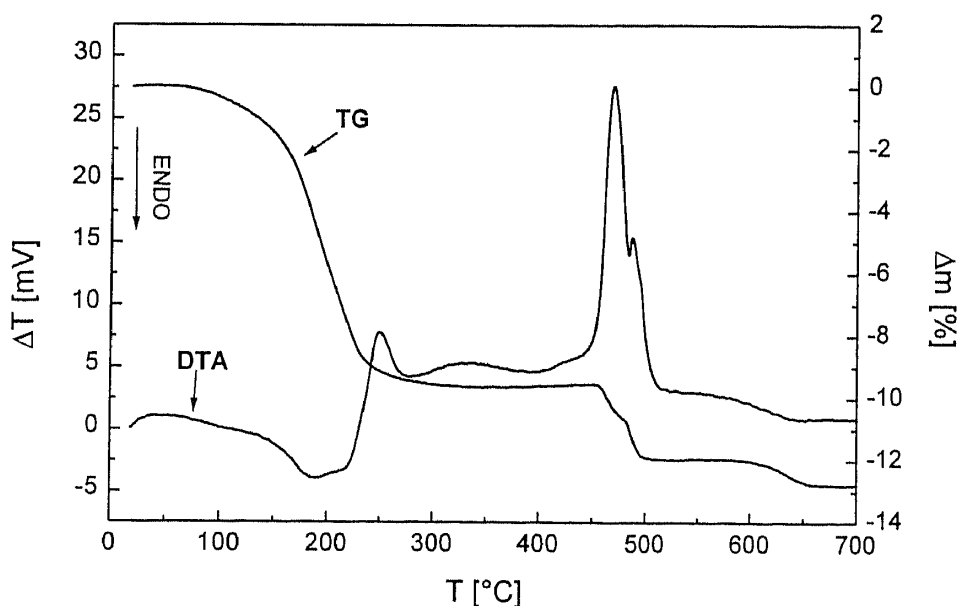


Fig. 1. Typical DTA-TG of a pure Nb_2O_5 xerogel (ethanolic sol), rate 10 K/min.

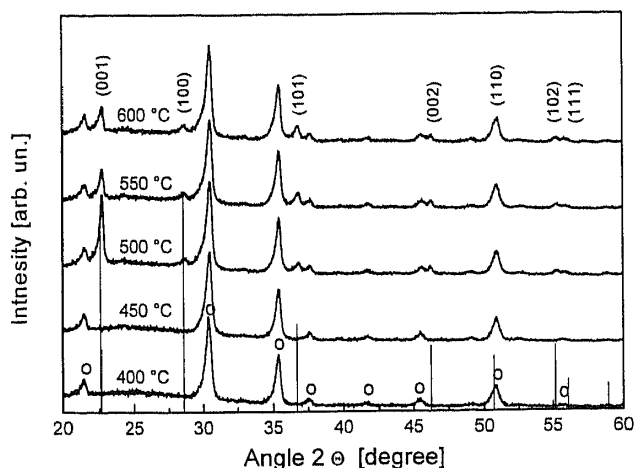


Fig. 2. X-ray diffraction spectra of pure Nb_2O_5 sintered between 400 and 600°C. O: ITO peaks, vertical lines: hexagonal Nb_2O_5 from JCPDS 28-317 data.

fragments of organic molecules (C_xH_y) and HCl [2,4], it is attributed to the building up of the inorganic amorphous network. The group of two exothermic peaks observed between 450 and 500°C accompanies the crystallization process (see also Fig. 2). A lower mass loss is also observed mainly due to the evolution of HCl. The overall DTA-TG behavior of doped xerogels is similar: an exothermic peak at $\sim 250^\circ\text{C}$ and a group of three exothermic peaks between 350 and 510°C for $\text{Nb}_2\text{O}_5:\text{Li}$ and Ti and a single one between 480 and 540°C for $\text{Nb}_2\text{O}_5:\text{Mo}$.

The thickness of the dip-coated single layers was found to depend on the amount and type of doping. It varies from (64 ± 4) nm for pure Nb_2O_5 (sol viscosity $\nu = 2.38 \text{ mm}^2/\text{s}$) to about 105 nm for a highly doped system (e.g. $\text{Mo}:\text{Nb} = 0.3$, $\nu = 2.54 \text{ mm}^2/\text{s}$).

Fig. 2 shows XRD plots of pure Nb_2O_5 -coatings. At $T < 450^\circ\text{C}$ the coatings are amorphous. At $T = 500^\circ\text{C}$ the coatings are crystalline, with a hexagonal structure (JCPDS 28-317 data). They are highly textured but the degree of orientation decreases with the sintering temperature.

In doped materials different structures have been obtained depending on the concentration and the sintering temperature [2,4]. Nb_2O_5 doped with Zr or Sn (up to 10%) present the same structures observed with the pure Nb_2O_5 . All $\text{Nb}_2\text{O}_5:\text{Li}$ are amorphous at 450°C. At 500°C an LiNb_3O_8 phase (JCPDS 26-1176 data) is observed with the less doped coatings ($< 10\%$), but with a higher concentration the samples remain amorphous. At $T = 600^\circ\text{C}$ all coatings are crystalline and consist of a mixture of a monoclinic LiNb_3O_8 and a hexagonal Nb_2O_5 phase.

Four different structures are observed in $\text{Nb}_2\text{O}_5:\text{Ti}$. All samples are amorphous at $T = 450^\circ\text{C}$. At low doping ($< 10\%$) only the Nb_2O_5 hexagonal structure is observed at $T > 500^\circ\text{C}$. For higher doping the coatings

are still amorphous at 500°C, but at 600°C we observed either a mixture of the Nb_2O_5 hexagonal structure and an orthorhombic structure $\text{Ti}_2\text{Nb}_{10}\text{O}_{29}$ ($\text{Ti}:\text{Nb} = 0.2$) or a pure $\text{Ti}_2\text{Nb}_{10}\text{O}_{29}$ phase ($\text{Ti}:\text{Nb} = 0.3$) (JCPDS 13-316 data). Four different structures have been also observed in $\text{Nb}_2\text{O}_5:\text{Mo}$. At 450°C the low doped coatings ($\text{Mo}:\text{Nb} = 5\%$) are already crystalline (hexagonal Nb_2O_5) and those with $\text{Mo}:\text{Nb} > 0.1$ crystallize with the $\text{Nb}_{12}\text{O}_{29}$ orthorhombic structure (JCPDS 34-1169 data). These phases are observed up to 500°C. A mixed structure of Nb_2O_5 and $\text{Nb}_{12}\text{O}_{29}$ is observed for all doped samples at 600°C, with a strong growth of the latter with the amount of doping.

The doping of Nb_2O_5 has, therefore, many effects on the structure and morphology of the coatings. Except for Mo doping the incorporation of foreign atoms pushed the crystallization temperature towards higher value, and when the concentration is high new crystalline phases appear either together with the hexagonal phase observed in pure Nb_2O_5 or alone.

The presence of these new phases also affects strongly the EC properties of the coatings. All amorphous coatings, irrespective of the sintering temperature, show a brown color under Li^+ insertion. Those crystallizing with a well-ordered hexagonal Nb_2O_5 phase (e.g. at 600°C pure Nb_2O_5 , all $\text{Nb}_2\text{O}_5:\text{Sn}$ or Zr, the low doped ($\leq 10\%$) $\text{Nb}_2\text{O}_5:\text{Ti}$) and those presenting a phase mixture with the predominance of the hexagonal Nb_2O_5 -phase (e.g. at 600°C all $\text{Nb}_2\text{O}_5:\text{Li}$, the low doped ($< 5\%$) $\text{Nb}_2\text{O}_5:\text{Mo}$) turn blue, and those presenting predominantly another phase (e.g. monoclinic LiNb_3O_8 ($\text{Nb}_2\text{O}_5:\text{Li}$), orthorhombic $\text{Ti}_2\text{Nb}_{10}\text{O}_{29}$ ($\text{Nb}_2\text{O}_5:\text{Ti}$) and orthorhombic $\text{Nb}_{12}\text{O}_{29}$ ($\text{Nb}_2\text{O}_5:\text{Mo}$)) exhibit a gray color. Typical spectra of the change of the optical density ΔOD reflecting these three colors are shown in Fig. 3 for $\text{Nb}_2\text{O}_5:\text{TiO}_2$ coatings.

The phases themselves are probably not important. The color seems to be related to the crystallite size (or the degree of crystallinity) of the coatings. All amorphous coating show a brown color, and the maximum of the absorption band lies around 400 nm. The gray color due to an almost flat absorption band in the visible with a maximum at about 500 nm is observed when the crystallite size is small, typically between 4 and 25 nm. The absorption band shifts towards larger wavelength ($\lambda \approx 1.1 \mu\text{m}$) when the structure is well crystallized with crystallite size larger than 40 nm and the color of the coating is blue (Fig. 4). In WO_3 layers, the absorption band for the amorphous structure is narrower than that of the crystalline structure and the position of the maximum shifts to lower wavelengths (900–1400 nm). This similarity between Nb_2O_5 and WO_3 allows us to propose the same absorption mechanism as already discussed by Wittwer et al. [5]. The absorption mechanism for the brown color is thought to arise from a polaron absorption. As the crystalline

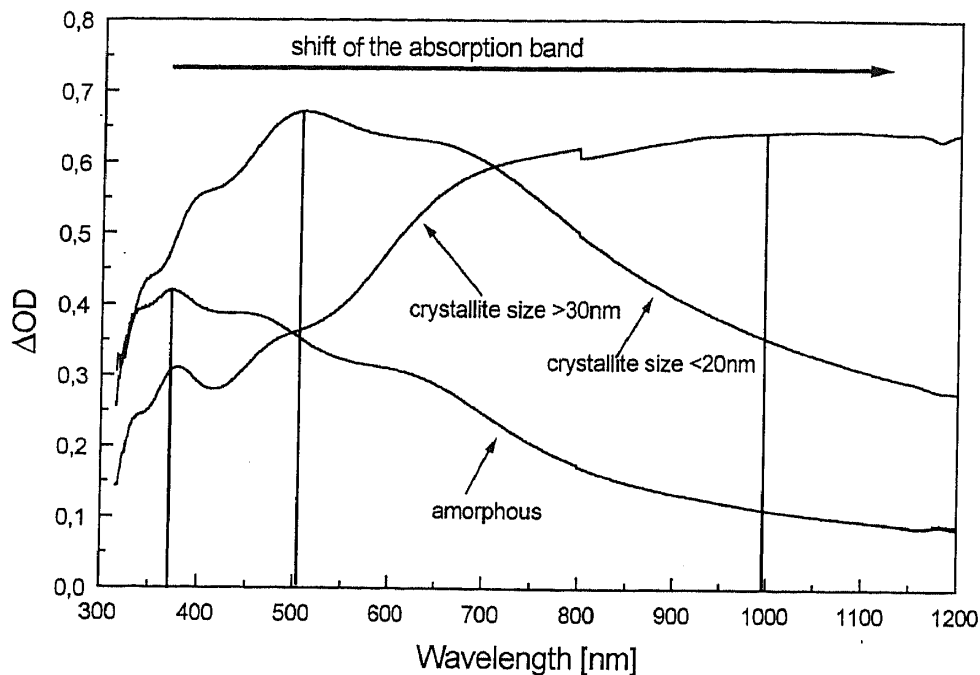


Fig. 3. Change in optical density observed with $\text{Nb}_2\text{O}_5:\text{Ti}$ coatings after Li^+ insertion: 120 s, -2.2 V, $+1$ V. The absorption bands give rise to a brown color ($\text{Ti:Nb} = 0.1$ amorphous state, 450°C), a gray color ($\text{Ti:Nb} = 0.3$, 600°C orthorhombic $\text{Ti}_2\text{Nb}_{10}\text{O}_{29}$) and a blue color ($\text{Ti:Nb} = 0$, 600°C , hexagonal Nb_2O_5).

order increases the absorption band becomes broader and shifts towards larger wavelength giving rise to a gray color. The blue color can probably be explained by the Drude model where the absorption is essentially governed by interaction with free electrons giving rise to a high reflection.

Whatever the type and amount of doping and the sintering temperature, the EC properties studied up to 5000 cycles have been found very stable (Fig. 5).

The amount of Li^+ ions which can be incorporated into the layers during a chronoamperometry cycle and consequently the deepness of the color is dependent on the amount of doping and the sintering temperature. However, the coloration efficiency η was always found to lay between 16 and $28 \text{ cm}^2/\text{C}$.

The highest $\Delta\tau$ measured at 550 nm (deepest color) has been obtained with the layers summarized in Table 1.

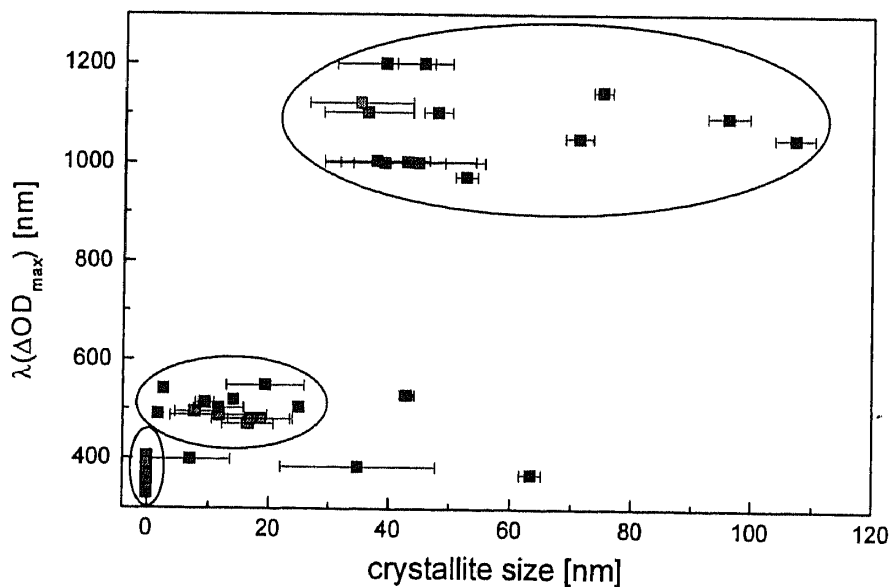


Fig. 4. Wavelength of the maximum of the change in optical density after Li^+ insertion (ΔOD) vs. crystallite size of all undoped or all doped Nb_2O_5 coatings studied between 400 and 600°C .

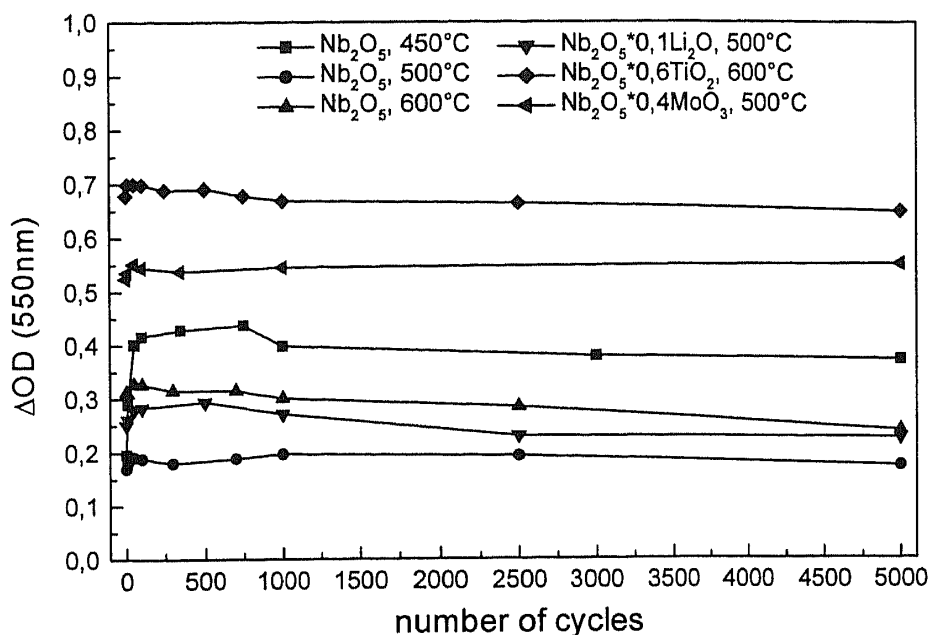


Fig. 5. Evolution of the change in optical density for a few coatings measured at 550 nm up to 5000 chronoamperometry cycles (120 s between -2.2 and $+1$ V vs. Ag/AgClO_4).

An important parameter to be considered to build complete EC cells is the Fermi potential of the EC and IS layers. Fig. 6 shows that for pure Nb_2O_5 the potentials increase significantly with the sintering temperature. They remain similar for Li and Ti doped materials but are significantly lower for Mo doping. Within a safe voltage range of ± 2.5 V, in which no chemical reaction will occur with the used electrolyte, all EC layers can incorporate a large amount of Li^+ ions up to $x \approx 1$. This is not the case for the $\text{TiO}_2\text{-CeO}_2$ IS electrode. The behavior of the potential as a function of the amount of Li^+ doping is quite different, and only a value $x \approx 0.14$ can be incorporated within the safe voltage range.

3.2. EC cells

Most of the complete devices reported till now use WO_3 as the EC electrode. The properties of the only complete cell using a niobia EC electrode was reported by Orel et al. [6]. The device was built with an

$\text{Nb}_2\text{O}_5\text{:Li}$ ($\text{Li}/\text{Nb} = 0.1$) coating sintered at 500°C as the EC electrode and an $\text{SnO}_2\text{:Sb:Mo}$ coating as the IS electrode. It exhibited a gray color with a transmission at 550 nm varying from 65 to about 20%. Due to the high switching voltages required to color this cell (-4 , $+2$ V) its lifetime was smaller than 500 cycles.

The cells reported here have the configuration glass/FTO/ $\text{Nb}_2\text{O}_5\text{:X}$ /liquid electrolyte/ $\text{TiO}_2\text{-CeO}_2$ /FTO/glass with the following EC electrodes: Nb_2O_5 (sintered at 450°C , 600°C), $\text{Nb}_2\text{O}_5\text{:Li}$ ($\text{Li}:\text{Nb} = 0.1$, 500°C), $\text{Nb}_2\text{O}_5\text{:Ti}$ ($\text{Ti}:\text{Nb} = 0.3$, 600°C), $\text{Nb}_2\text{O}_5\text{:Mo}$ ($\text{Mo}:\text{Nb} = 0.2$, 500°C). They have been switched within the safe voltages of ± 2.5 V. All cells colored under Li^+ ions insertion but the highest coloring change was obtained using the $\text{Nb}_2\text{O}_5\text{:Mo}$ electrode.

According to a model developed by Bullock et al. [7] the internal chemical potential difference (emf) of the EC and IS electrodes, the ratio $r = (\rho_{\text{EC}} \cdot d_{\text{EC}}) / (\rho_{\text{IS}} \cdot d_{\text{IS}})$, where ρ is the molar density and d is the thickness of the layers, as well as the maximum value of the amount of Li which can be incorporated in the layers, are

Table 1

Summary of the parameters giving rise to the highest (OD measured after a chronoamperometry cycle (120 s, -2.2 V, $+1$ V vs. Ag/AgClO_4). The coating thickness is about 180 nm.

Color	Layer	X:Nb	$T_{\text{sintering}}$ ($^\circ\text{C}$)	$\Delta\tau$	η (cm^2/C)
Brown	$\text{Nb}_2\text{O}_5\text{:Li}$	0.1	450	0.45	16
Gray	$\text{Nb}_2\text{O}_5\text{:Ti}$	0.2; 0.3	600	0.55	27
	$\text{Nb}_2\text{O}_5\text{:Mo}$	0.2	450, 500	0.60	21.5
Blue	Nb_2O_5	-	600	0.53	17

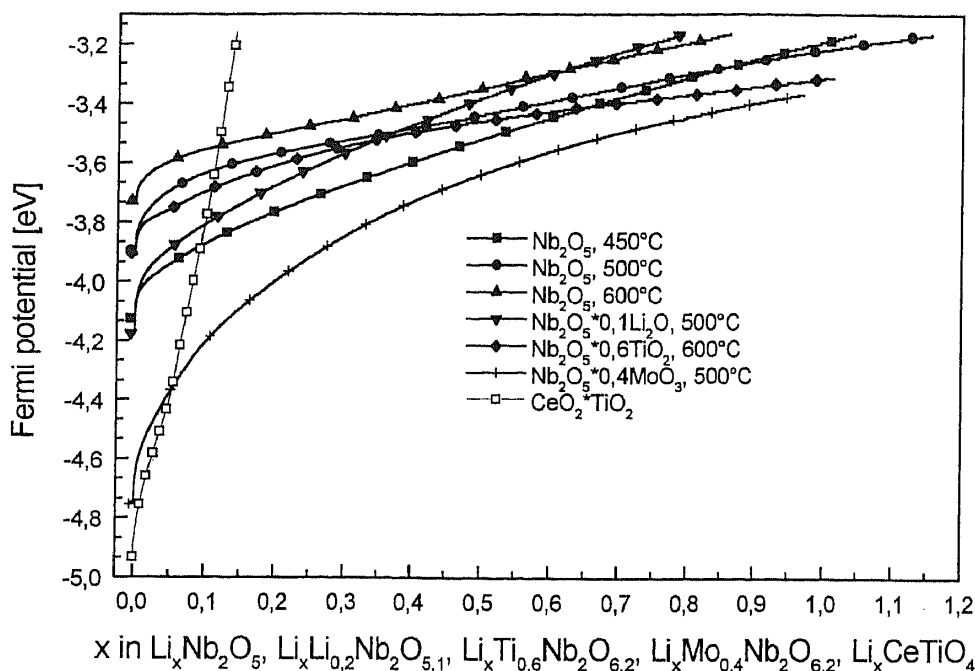


Fig. 6. Fermi potential curves determined from coulometric titration using a $5 \mu\text{A}/\text{cm}^2$ current density after 50 chronoamperometric cycles for different pure and doped Nb_2O_5 as well as for a TiO_2 - CeO_2 IS layer.

important to design a complete cell. This model was applied to the five cells using a value $y = 0.14$ for the $\text{Li}_x\text{TiCeO}_4$ layer and r values varying from 0.88 to 1.15 [2,8]. The results confirm that the use of the Nb_2O_5 :Mo coating is strongly favored (more adequate internal emf than with the other layers) and that the photopic transmittance variations $\Delta\tau$ will increase with the decrease of the thickness ratio $d_{\text{EC}}/d_{\text{IS}}$. This implies that the IS electrode should be much thicker than the ES electrode.

Fig. 7 shows the experimental change of the photopic transmission $\Delta\tau$ obtained with the 180-nm thick Nb_2O_5 :Mo EC electrode and four different thicknesses of the TiO_2 - CeO_2 electrode ($r = 0.67$ for one layer, 0.33 for two layers, 0.22 for three layers and 0.17 for four layers). This model has been partly confirmed. $\Delta\tau$ for two IS layers is higher than for one layer, but the value saturates for higher thicknesses. This is probably due to a very high ohmic resistance of the IS electrode when the thickness becomes larger than 400–500 nm which introduces a large ohmic drop not included in the calculation. The use of three or four IS layers only improves the lifetime of the cell. The highest amount of charge exchanged was $18 \text{ mC}/\text{cm}^2$ (three IS layers) and the maximum change in the transmission was $\Delta\tau = 0.28$. The best cells were stable up to 20,000 cycles. The deterioration of the cells is probably due to a corrosion effect between the liquid electrolyte and the IS electrode.

4. Conclusions

Pure and Sn, Zr, Li, Ti, Mo doped Nb_2O_5 coatings have been prepared by the sol-gel process. All layers exhibit EC properties when Li^+ ions are intercalated. The type of ions and the sintering temperature has a

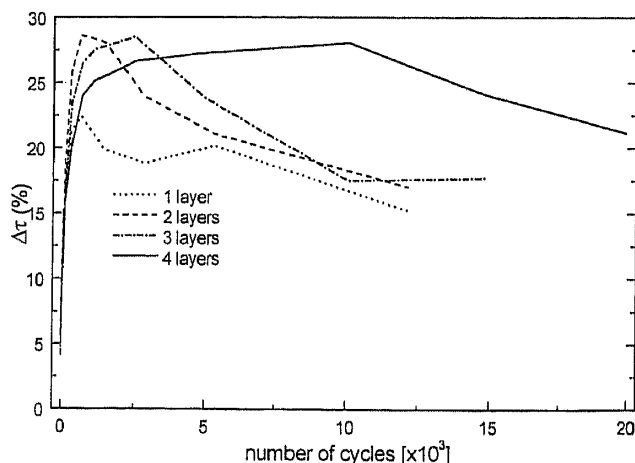


Fig. 7. Change of light transmittance $\Delta\tau$ calculated according to DIN EN 410 (weighted with the relative light function D_{65} and the human eye sensibility for daylight $V(\lambda)$) vs. the number of cycles of $6 \times 8 \text{ cm}^2$ devices made with a 180-nm thick Nb_2O_5 :0.4 Mo EC electrode and a TiO_2 - CeO_2 IS electrode having a thickness varying between 240 nm (one layer) to approx. 950 nm (four layers). Applied voltage: -2.5 V ; $+2.5 \text{ V}$ each during 120 s.

large influence on the structure, morphology and electrochemical behavior. Amorphous layers present a brown color, crystalline layers with small crystallite size (5–20 nm) color gray and those with larger crystallite size (35–100 nm) a blue color. The properties of the layers giving the highest change of the optical density have been discussed. EC cells using pure and doped niobia as the EC electrode and $\text{TiO}_2\text{--CeO}_2$ as counterelectrode have been built and characterized. Cells made with $\text{Nb}_2\text{O}_5\text{:Mo}$ layers sintered at 500°C and switched between ± 2.5 V up to 20,000 cycles exhibit the highest photopic transmittance change $\Delta\tau = 0.28$.

References

- [1] M.A. Aegerter, Sol-gel niobium pentoxide: a promising material for electrochromic coatings, batteries, nanocrystalline solar cells and catalysis, *Solar Energy Materials & Solar Cells*, 2001
- [2] M. Schmitt, PhD thesis, University of Saarland, 2000.
- [3] B. Munro, P. Conrad, S. Krämer, H. Schmidt, P. Zapp, *Solar Energy Materials & Solar Cells* 54 (1998) 131.
- [4] M. Schmitt, M.A. Aegerter, in: C.M. Lampert (Ed.), *Switchable Materials and Flat Panel Displays*, vol. 3788, SPIE, Bellingham, WA, 1999, pp. 93–102.
- [5] V. Wittwer, O.F. Schirmer, P. Schlotter, *Solid State Communications* 25 (1978) 977.
- [6] B. Orel, U. Opara Krasovec, M. Macek, F. Svegl, U. Lavrencic Stangar, *Solar Energy Materials & Solar Cells* 56 (1999) 343.
- [7] J.N. Bullock, H.M. Branz, in: C.M. Lampert (Ed.), *Optical Materials Technology for Energy Efficiency and Solar Energy Conversion XIV*, vol. 2531, SPIE, Bellingham, WA, 1995, pp. 152–160.
- [8] M. Schmitt, M.A. Aegerter, in: C.M. Lampert (Ed.), *Switchable Materials and Flat Panel Displays*, vol. 3788, SPIE, Bellingham, WA, 1999, pp. 75–83.